International Journal of Applied Electromagnetics and Mechanics 42 (2013) 349–358
DOI 10.3233/JAE-131669
IOS Press


# Electromagnetic scattering of metallic cylinders of arbitrary shape by using asynchronous particle swarm optimization and non-uniform steady state genetic algorithm

Ching-Lieh Li[a], Chi-Hsien Sun[b], Chien-Ching Chiu[a,*], Lung-Fai Tuen[a] and Chien-Hua Su[a]
[a]*Electrical Engineering Department, Tamkang University, New Taipei City, Taiwan*
[b]*Department of Electronic and Computer Engineering, National Taiwan University of Science and Technology, Taipei City, Taiwan*

**Abstract.** Two techniques for the shape reconstruction of multiple metallic cylinders from scattered fields are investigated in this paper, in which two-dimensional configurations are involved. After an integral formulation, the method of moment (MoM) is applied to solve it numerically. Two separate perfect-conducting cylinders of unknown shapes are buried in one half-space and illuminated by the transverse magnetic (TM) plane wave from the other half space. Based on the boundary condition and the measured scattered field, a set of nonlinear integral equation is derived and the imaging problem is reformulated into optimization problem. The non-uniform steady state genetic algorithm (NU-SSGA) and asynchronous particle swarm optimization (APSO) are employed to find out the global extreme solution of the object function. Numerical results demonstrate even when the initial guesses are far away from the exact shapes, and the multiple scattered fields between two conductors are serious, good reconstruction can be obtained. In addition, the effect of Gaussian noise on the reconstruction results is investigated and the numerical simulation shows that the reconstruction results are good and acceptable, as long as the SNR is greater than 20 dB.

Keywords: Inverse scattering, microwave image, buried conductors, asynchronous particle swarm optimization, genetic algorithms (SSGA), half space

## 1. Introduction

The solution of an electromagnetic inverse scattering problem has been an area of research for many years because of its wide variety of applications which include, for example, geological investigations of the earth structure, nondestructive evaluation and characterization of different food grains, imaging of human organs in biomedical microwave tomography, ground-penetrating radar, and possible detection

*Corresponding author: Chien-Ching Chiu, Electrical Engineering Department, Tamkang University, New Taipei City, Taiwan. E-mail: chiu@ee.tku.edu.tw.

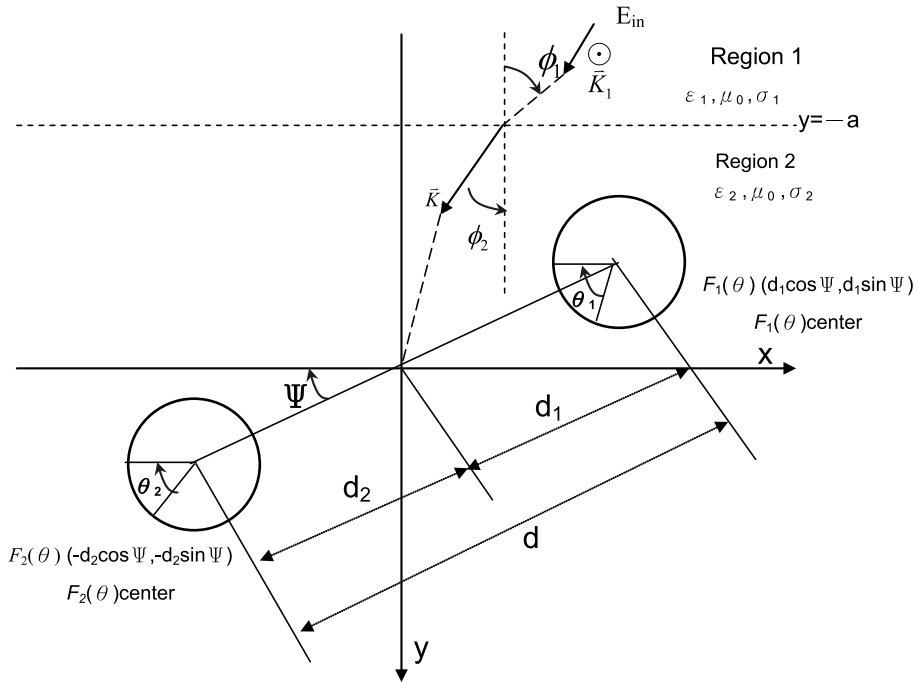


Fig. 1. Geometry of two perfectly conducting cylinders in $(x, y)$ plane.

of diseases in trees and forests etc. [1–7]. Furthermore, the inverse problems related to the underground objects are of particular importance in scattering theory. However, inverse problems of this type are difficult to solve because they are nonlinearity [8,9].

One way for the nonlinear inverse problem is solving the forward scattering problem iteratively to minimize an error function known as the objective function. This function represents the error between the measured scattered fields and the simulated fields during the updates of the evolving objects in each inversion [10–30]. Recently, several papers for inverse scattering problems have been published on the subject of 2-D object about deal with shape reconstruction problems by using the Newton-Kantorvoitch method [31]. However, for a gradient-type method, it is well known that the convergence of the iteration depends highly on the initial guess. If a good initial guess is given, the speed of the convergence can be very fast. On the other hand, if the initial guess is far away from the exact one, the searching tends to get fail [13]. In general, they tend to get trapped in local minima when the initial trial solution is far away from the exact one. Thus, some population-based stochastic methods, such as genetic algorithms (GAs) [10,12,13,17–21], differential evolution (DE) [11,22–27], particle swarm optimization (PSO) [26–29], subspace-based optimization method [32], Neural network [33] and level-set algorithm [34] are proposed to search the global extreme of the inverse problems to overcome the drawback of the deterministic methods.

In general, most of objects are placed in a homogeneous space, while Chiu and Chen [35,36] reconstruct a buried imperfectly conducting cylinder by genetic algorithm. The microwave imaging of multiple objects in free space has been proposed by Chiu [37]. Qing [38] has been proposed using differential evolution strategy with individuals in groups (GDES) to solve the multiple conductor problem. This paper is based on our earlier work on inverse scattering where the NU-SSGA is utilized to reconstruct the buried perfect conductor cylinders [39]. Moreover, to the best of our knowledge, there are still

no numerical results by APSO to reconstruct the multiple conductors. Moreover, a comparative study about the performances of APSO and NU-SSGA to inverse scattering problems is also investigated. In Section 2, a theoretical formulation for the inverse scattering is presented. The general principles of optimization algorithms and the way we applied them to the inverse problem are described. Numerical results for reconstructing objects of different shapes with noise are given in Section 3. Finally, some conclusions are drawn in Section 4.

## 2. Theoretical formulation

Let us consider two separate perfectly conductors buried in a lossy homogeneous half-space, as shown in Fig. 1. The media in regions 1 and 2 are characterized by the permittivities and the conductivities ($\varepsilon_1$, $\sigma_1$) and ($\varepsilon_2$, $\sigma_2$), respectively, while the permeability $\mu_0$ is used for each region, i.e., only nonmagnetic media are concerned here. There are two separate conducting cylinders with cross section that are described by polar coordinates in the xy plane through shape equations $\rho = F(\theta)$, in other word, the objects are star-like shapes. The conductors are illuminated by TM (transverse magnetic) plane wave with time dependence $e^{j\omega t}$ on region 1, in which the electric field is assumed parallel to the $z$-axis. Let $E_{in}$ denote the incident field from region 1 to region 2 with the incident angle $\Phi_1$. Due to the interface between region 1 and region 2, the incident plane wave generates two waves in the interface, which would exist in the absence of the conducting targets: the reflected wave in the region 1 and the transmitted wave in the region 2. Thus the unperturbed field is given by

$$\overrightarrow{E_i} = E_i(x,y)\hat{z} \tag{1}$$

with Eq. (1), where

$$E_i(x,y) = \begin{cases} E_1 = e^{-jk_1[x\sin\phi_1+(y+a)\cos\phi_1]} + R_1 e^{-jk_1[x\sin\phi_1-(y+a)\cos\phi_1]}, & y \leqslant -a \\ E_2 = Te^{-jk_2[x\sin\phi_2+(y+a)\cos\phi_2]}, & y > -a \end{cases}$$

where

$$R_1 = \frac{1-n}{1+n}, T = \frac{2}{1+n}, n = \frac{\cos\phi_2}{\cos\phi_1}\sqrt{\frac{\varepsilon_2 - j\frac{\sigma_2}{\omega}}{\varepsilon_1 - j\frac{\sigma_1}{\omega}}}$$

$k_1\sin\phi_1 = k_2\sin\phi_2, k_i^2 = \omega^2\varepsilon_i\mu_0 - j\omega\mu_0\sigma_i, \mathrm{Im}(k_i) \leqslant 0, i = 1,2.$

We introduce an equivalent induced current concept, and then the scattered field in each region can be expressed by

$$E_S(x,y) = \begin{cases} -\int_0^{2\pi} G_1(x,y,F_1(\theta'),\theta')J_1(\theta')d\theta' - \int_0^{2\pi} G_1(x,y,F_2(\theta'),\theta')J_2(\theta')d\theta', & y \leqslant -a \\ -\int_0^{2\pi} G_2(x,y,F_1(\theta'),\theta')J_1(\theta')d\theta' - \int_0^{2\pi} G_2(x,y,F_2(\theta'),\theta')J_2(\theta')d\theta', & y > -a \end{cases} \tag{2}$$

In Eq. (2), the current density and Green's functions are given by

$$J_h(\theta_h') = -j\omega\mu_0\sqrt{F_h^2(\theta_h') + (F_h'(\theta_h'))^2}J_{sh}(\theta_h')$$

$$G(x,y,F_h(\theta'),\theta') = \begin{cases} G_1(x,y,F_h(\theta'),\theta'), & y \leqslant -a \\ G_2(x,y,F_h(\theta'),\theta') = G_f(x,y,F_h(\theta'),\theta') + G_S(x,y,F_h(\theta'),\theta'), & y > -a \end{cases} \tag{3}$$

$h = 1,2$. Please see [39] for details.

The inverse scattering problem is to determine the shapes and positions of the conducting cylinders when the scattered electric field $E_S$ is measured outside the scatterer. For shape expansions, the Fourier series is selected to express the shape functions. Assume the approximate center of the scatterer, which in fact can be any point inside the scatterer, is known. The shape functions $F_1(\theta)$ and $F_2(\theta)$ can be expanded by Fourier series as follows:

$$F_1(\theta) = \sum_{n=0}^{N/2} B_{1n}\cos(n\theta) + \sum_{n=1}^{N/2} C_{1n}\sin(n\theta) \tag{4}$$

$$F_2(\theta) = \sum_{n=0}^{N/2} B_{2n}\cos(n\theta) + \sum_{n=1}^{N/2} C_{2n}\sin(n\theta) \tag{5}$$

where $B_{1n}$, $C_{1n}$, $B_{2n}$ and $C_{2n}$ are real coefficients to be determined and $2(N+1)$ is the number of unknowns for expanding the shape functions. Note that the discretization number of $J(\theta)$ for the inverse problem must be different from that for the direct problem. In our study, the discretization of the current density for the direct problem is twice of that for the inverse problem. Since it is crucial that the synthetic data generated by the direct solver are not alike those obtained through the inverse solver. This problem is resolved by an optimization approach, for which the global searching scheme SSGA, APSO is employed to minimize the following objective function (*OF*):

$$OF = \left\{ \frac{1}{M_t} \sum_{m=1}^{M_t} \left| E_s^{\exp}(\bar{r}_m) - E_s^{cal}(\bar{r}_m) \right|^2 \Big/ \left| E_s^{\exp}(\bar{r}_m) \right|^2 \right\}^{1/2} \tag{6}$$

where $M_t$ is the total number of measured points. $E_s^{\exp}(\bar{r})$ and $E_s^{cal}(\bar{r})$ are the measured scattered field and the calculated scattered field, respectively. The smaller the *OF*, the smaller the error of the scattering field such that the reconstructed shapes are closed to exact one.

### *2.1. A synchronous particle swarm optimization (APSO)*

Clerc [40] suggested the use of a different velocity update rule, which introduced a parameter $\xi$ called constriction factor. The role of the constriction factor is to ensure convergence when all the particles tend to stop their movement.

The velocity update rule is then given by

$$v_j^{k+1} = \xi \cdot \left( v_j^k + c_1 \cdot \phi_1 \cdot \left( x_{pbest_j}^k - x_j^k \right) + c_2 \cdot \phi_2 \cdot \left( x_{gbest}^k - x_j^k \right) \right) \tag{7}$$

$$x_j^{k+1} = x_j^k + v_j^{k+1}, \quad j = 0 \sim N_p - 1 \tag{8}$$

where

$$\xi = \frac{2}{\left| 2 - \phi - \sqrt{\phi^2 - 4\phi} \right|}, \phi = c_1 + c_2 \geqslant 4.$$

By Eq. (7), particles fly around in the multidimensional solution space and adjust their positions according to their own experience and the experience of neighboring particles, by exploiting the knowledge of best positions encountered by themselves and their neighbors.

The key distinction between a particle swarm optimization (PSO) and the asynchronous particle swarm optimization (APSO) is on the updating mechanism, damping boundary condition and mutation scheme. In the typical synchronous PSO, the algorithm updates all the particles velocities and positions using Eq. (7) at the end of each generation. And then update the best positions, $x_{pbest}$ and $x_{gbest}$. Alternatively, the current updating mechanism of asynchronous PSO use the following rule: just after the update by Eq. (7) for each particle the best positions $x_{pbest}$ and $x_{gbest}$ will be replaced if the new position is better than the current best ones such that they can be used immediately for the next particle. In this way, the swarm reacts more quickly to speedup the convergence.

In this paper we have applied the damping boundary condition and mutation scheme. The mutation scheme plays a role in avoiding premature convergences for the searching procedure and helps the $x_{gbest}$ escape from the local optimal position.

### *2.2. Non-uniform steady-state genetic algorithm (NU-SSGA)*

The non-uniform steady-state genetic algorithm (NU-SSGA) was developed and first applied into inverse scattering problem by Chiu in 2004 [41]. The SSGA is very powerful stochastic global optimization methods based on genetic recombination and evaluation in nature. In general, the SSGA must be able to perform seven basic tasks:

1. Encode the solution parameters as genes.
2. Create a string of the genes to form a chromosome.
3. Initialize a starting population.
4. Evaluate and assign fitness values to individuals in the population.
5. Perform reproduction through some selection scheme.
6. Perform recombination of genes to produce offspring.
7. Perform mutation of genes to produce offspring.

The key distinction between an SSGA and a typical GAs is in the number of fitness calculation. In a typical GAs, each generation of the algorithm replaces the population with the new population. On the contrary, SSGA only needs to generate a few offspring, by non-uniform beta distribution in crossover and mutation, to replace the weakest individual in each new generation. The non-uniform probability density scheme in genetic operator could increase the searching diversity in the early iteration, and also increase the exploration ability of the algorithm in latter iteration. In other words, the number of fitness calculation corresponding to the new population is large in a typical SSGA compared with NU-SSGA. To prevent the superior individual from been lost during the NU-SSGA optimization process, the rank scheme is employed in the selection operation for which copies the superior individual to the next generation. Based on the characteristic of NU-SSGA in reducing the numbers of fitness calculation, we are able to reconstruct the microwave image efficiently. The details see [42]. It should be noted that the shape function used to describe the shape of the cylinder will be determined by the APSO and NU-SSGA scheme.

## 3. Numerical results

Let us consider two separate perfectly conducting cylinders which are immersed in a lossless half-space ($\sigma_1 = \sigma_2 = 0$). The permittivities in region 1 and region 2 are characterized by $\varepsilon_1 = \varepsilon_0$ and $\varepsilon_2 = 2.56\varepsilon_0$, respectively, and the permeability $\mu_0$ is used for each region which are only nonmagnetic

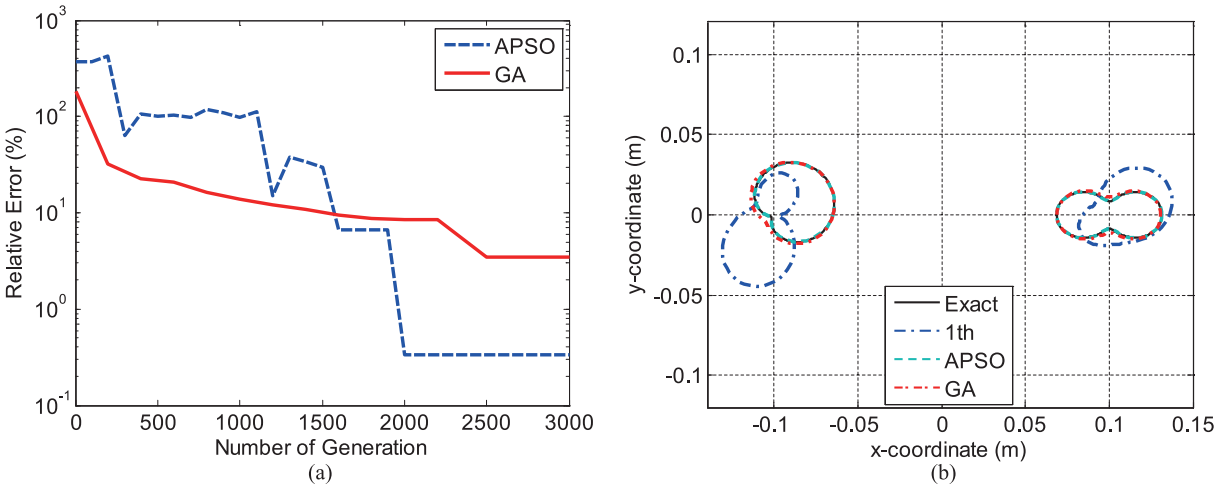


Fig. 2. (a) The reconstructed shapes for example 1. The solid curves represent exact shapes, and other curves are the calculated shapes APSO and NU-SSGA in final generation, respectively. (b) The error of the reconstructed shapes in each generation.

media. A TM polarization plane wave of unit amplitude is incident from region 1 to region 2 as shown Fig. 1. The frequency of the incident wave is chosen to be 3 GHz. For all simulation, we set the position of the interface at $y = -a$, and the two objects are buried at the same depths ($a \cong \lambda_0$). In our experiment, the scattered fields are measured on a probing line along $y = -(a+0.01)$ m in region 1. The two targets are illuminated by three waves with incident angles. g That are 0°, 45° and 315°, respectively, and then the 8 measurements at equally separate points are used along $y = -(a + 0.01)$ for each incident angle. Therefore there are totally 24 measurements in each simulation. Here, the parameter is set to 0.1 m in all simulation.

There are fourteen unknown parameters to retrieve. The relative coefficient of the modified APSO are set as below: The learning coefficients $c_1$ and $c_2$, are set to 2.8 and 1.3, respectively [43].

The relative coefficients of the NU-SSGA are set as below: the crossover probability $p_c$ and the mutation probability $p_m$ are set to 0.1 and 0.08, respectively [42]. The former 0.1 is to maintain the concept of steady state, the latter 0.08 is suitable to avoid premature convergence in our experience.

The first example, the shape functions are chosen to be $F_1(\theta) = [0.02 + 0.0115\cos(2\theta)]$ m and $F_2(\theta) = [0.02 + 0.015\cos(\theta) + 0.01\sin(\theta)]$ m, respectively. The $d_1$, $d_2$ and $\Psi$ are 0.1 m, 0.1 m and 0°, respectively. This example shows to reconstruct the different shape functions. The reconstructed shape functions are plotted in Fig. 2(a). Moreover, the relative error of the reconstructed shapes versus numbers of generation shown in Fig. 2(b). The APSO and NU-SSGA relative error are about 0.2% and 2.5% in the final, respectively. Here, relative error (RE) is defined as following

$$RE = \frac{1}{2N'}\sum_{i=1}^{N'}\left[\frac{\left|F_1^{cal}(\theta_i) - F_1(\theta_i)\right|}{F_1(\theta_i)} + \frac{\left|F_2^{cal}(\theta_i) - F_2(\theta_i)\right|}{F_2(\theta_i)}\right] \tag{9}$$

where $N'$ is set to 360. The quantities relative error provides measures of how well $F_1^{cal}(\theta)$ and $F_2^{cal}(\theta)$ approximate $F_1(\theta)$ and $F_2(\theta)$, respectively. It is clear that the reconstructed results are good although the reconstructed shapes of the initial generation are far away from exact ones.

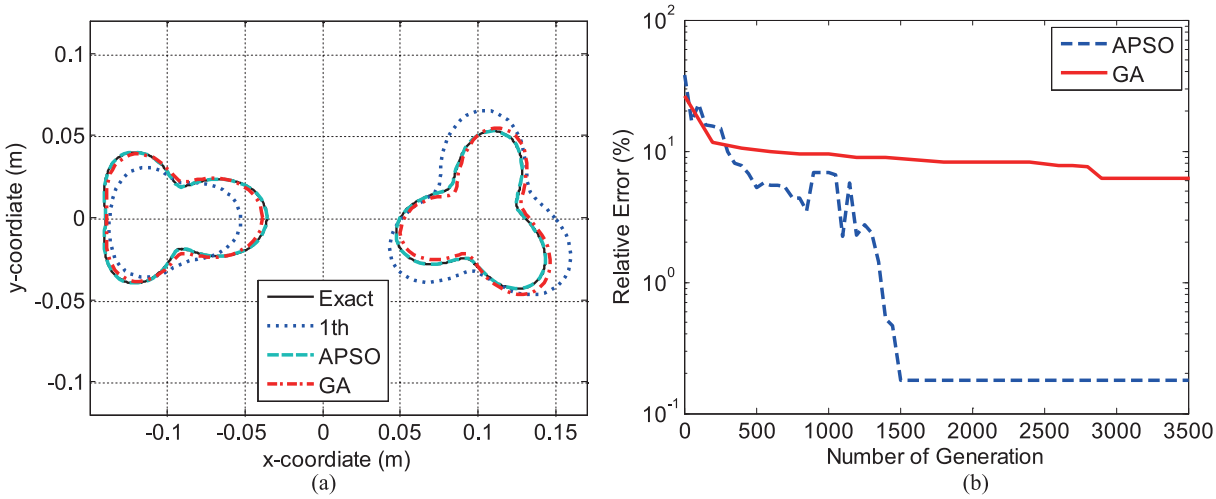


Fig. 3. (a) The reconstructed shapes for example 2. The solid curves represent exact shapes, and other curves are the calculated shapes APSO and NU-SSGA in final generation, respectively. (b) The error of the reconstructed shapes in each generation.

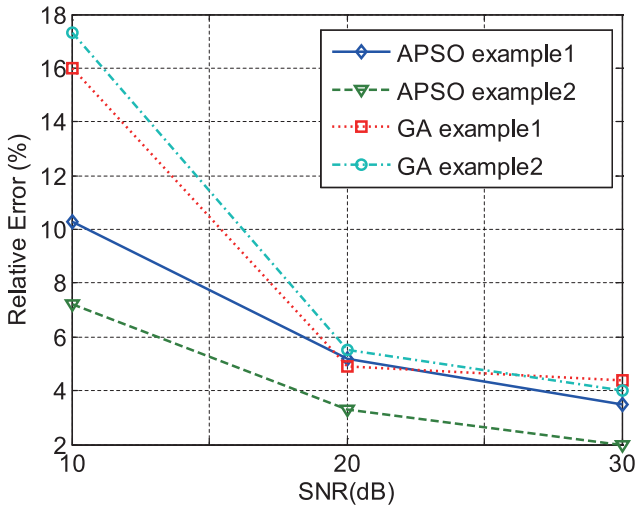


Fig. 4. The trend of relative error (RE) for example 1 and example2 with noise.

In the second example, two shape functions are selected to be $F_1(\theta) = [0.04 - 0.01\cos(3\theta) - 0.01\sin(3\theta)]$ m and $F_2(\theta) = [0.04 + 0.012\cos(2\theta) + 0.012\cos(3\theta)]$ m, respectively. Moreover, the $d_1$, $d_2$ and $\Psi$ are 0.1 m, 0.1 m and 0°, respectively. This example shows that the proposed scheme can reconstruct more complicated scatterers whose shape function for each target has three concavities. The reconstructed shape functions are plotted in Fig. 3(a). Moreover, The relative error of the reconstructed shapes versus numbers of generation shown in Fig. 3(b). The APSO and NU-SSGA relative error are about 0.01% and 6.2% in the final, respectively.

For investigating the effect of noise, Fig. 4 shows the reconstructed results for the multiple conductors cylinder under the condition that the recorded scattered fields are contaminated by noise, of which the SNR includes 30 dB, 20 dB and 10 dB. It is observed that good reconstruction can be obtained for the shape of the metallic cylinder when the SNR is above 20 dB.

## 4. Conclusions

This paper presents a study by using the steady state Asynchronous particle swarm optimization algorithm and genetic algorithm to reconstruct the shapes of two separate perfectly conducting buried cylinders through knowledge of scattered fields. The targets are illuminated by TM plane wave in region 1. Then based on the boundary condition and measured scattered field, we have derived a set of nonlinear integral equations and reformulated the inversion problem into an optimization problem. It should be noted that Fourier series expansion is employed to describe the shapes of the buried cylinders, which can be readily replaced by using the technique of cubic spline interpolation. Nevertheless, the shapes of the objects can be reconstructed by using the APSO and NU-SSGA from the scattered fields in region 1. Numerical results show that the APSO yields better reconstructed results as compared with those by GA. Finally, to mimic experiments the effects of white Gaussian noise on the reconstruction results is investigated, and the numerical result shows APSO yields better immunity against noise than NU-SSGA does.

## Acknowledgment

This work was supported by National Science Council, Republic of China, under Grant NSC 101-2221 -E-032-029-.

## References

[1] X. Chen, Subspace-based optimization method for solvinginverse-scattering problems, *IEEE Transactions on Geoscience and Remote Sensing* **48**(1) (Jan 2010), 42–49.
[2] A. Brancaccio and G. Leone, Multimonostatic shape reconstruction of two-dimensional dielectric cylinders by a Kirchhoff-based approach, *IEEE Transactions on Geoscience and Remote Sensing* **48**(8) (Aug 2010), 3152–3161.
[3] C.C. Chiu and C.H. Sun, Computational approach based on a differential evolution with self-adaptive concept for microwave imaging of two-dimensional inverse scattering problem, *Electromagnetics* **32**(8) (Nov 2012), 451–464.
[4] C.C. Chiu and C.H. Sun, A study of microwave imaging for a metallic cylinder, *International Journal of RF and Microwave Computer-Aided Engineering* **22**(5) (Sept 2012), 632–638.
[5] G. Oliveri, P. Rocca and A. Massa, A bayesian-compressive-sampling-based inversion for imaging sparse scatterers, *IEEE Transactions on Geoscience and Remote Sensing* **49**(10) (Oct 2011), 3993–4006.
[6] A.K. Hamid and F.R. Cooray, TE scattering by a perfect electromagnetic conducting semi-elliptic-cylindrical boss on a perfectly conducting plane, *International Journal of Applied Electromagnetics and Mechanics* **38**(1) (2012), 1–8.
[7] C.C. Chiu, C.H. Sun, C.L. Li and C.H. Huang, Comparative study of some population-based optimization algorithms on inverse scattering of a two-dimensional perfectly conducting cylinder in slab medium, *IEEE Trans Geosci Remote Sens* **51**(4) (Apr 2013), 2302–2315.
[8] P.C. Sabatier, Theoretical considerations for inverse scattering, *Radio Science* **18** (Jan 1983), 629–631.
[9] R.K. Singh, Effect of background magnetic field on the electron-bunching and saturation phenomenon in a gyro-TWT, *International Journal of Applied Electromagnetics and Mechanics* **38**(2–3) (2012), 157–164.
[10] W. Chien, C.H. Huang, C.C. Chiu and C.L. Li, Image reconstruction for 2D homogeneous dielectric cylinder using FDTD method and SSGA, *International Journal of Applied Electromagnetics and Mechanics* **32**(2) (Feb 2010), 111–123.
[11] A. Semnani, I.T. Rekanos, M. Kamyab and T.G. Papadopoulos, Two-dimensional microwave imaging based on hybrid scatterer representation and differential evolution, *IEEE Trans Antennas Propag* **58**(10) (Oct 2010), 3289–3298.
[12] C.H. Sun, C.L. Li, C.C. Chiu and C.H. Huang, Time domain image reconstruction for a buried 2D homogeneous dielectric cylinder using NU-SSGA, *Research in Nondestructive Evaluation* **22**(1) (Jan 2011), 1–15.
[13] T. Moriyama, Z. Meng and T. Takenaka, Forward-backward time-stepping method combined with genetic algorithm applied to breast cancer detection, *Microwave and Optical Technology Letters* **53**(2) (2011), 438–442.
[14] C.H. Chen, C.C. Chiu, C.H. Sun and W.L. Chang, Two-dimensional finite-difference time domain inverse scattering scheme for a perfectly conducting cylinder, *Journal of Applied Remote Sensing* **5** (May 2011), 053522.

[15] C.H. Sun, C.C. Chiu and C.J. Lin, Image reconstruction of inhomogeneous biaxial dielectric cylinders buried in a slab medium, *International Journal of Applied Electromagnetics and Mechanics* **34**(1–2) (Nov 2010), 33–48.
[16] M. Cayoren, I. Akduman, A. Yapar and L. Crocco, Shape reconstruction of perfectly conducting targets from single-frequency multiview data, *IEEE Geosci Remote Sens Lett* **5**(3) (Jul 2008–Jan 2009), 383–386.
[17] C.H. Sun, C.L. Liu, K.C. Chen, C.C. Chiu, C.L. Li and C.C. Tasi, Electromagnetic transverse electric wave inverse scattering of a partially immersed conductor by steady-state genetic algorithm, *Electromagnetics* **28**(6) (Aug 2008), 389–400.
[18] W. Chien, C.H. Sun and C.C. Chiu, Image reconstruction for a partially immersed imperfectly conducting cylinder by genetic algorithm, *International Journal of Imaging Systems and Technology* **19** (Dec 2009), 299–305.
[19] X.M. Zhong, C. Liao and W. Chen, Image reconstruction of arbitrary cross section conducting cylinder using UWB pulse, *Journal of Electromagnetic Waves Application* **21**(1) (2007), 25–34.
[20] W. Chien and C.C. Chiu, Using NU-SSGA to reduce the searching time in inverse problem of a buried metallic object, *IEEE Transactions on Antennas and Propagation* **53**(10) (Oct 2005), 3128–3134.
[21] A. Massa, D. Franceschini, G. Franceschini, M. Pastorino, M. Raffetto and M. Donelli, Parallel GA-based approach for microwave imaging applications, *IEEE Transaction on Antennas and Propagation* **53**(10) (Oct 2005), 3118–3127.
[22] A. Qing, Dynamic differential evolution strategy and applications in electromagnetic inverse scattering problems, *IEEE Transactions on Geoscience and Remote Sensing* **44**(1) (January 2006), 116–125.
[23] C.H. Sun, C.C. Chiu, C.L. Li and C.H. Huang, Time domain image reconstruction for homogenous dielectric objects by dynamic differential evolution, *Electromagnetics* **30**(4) (May 2010), 309–323.
[24] C.H. Sun, C.C. Chiu, W. Chien and C.L. Li, Application of FDTD and dynamic differential evolution for inverse scattering of a two – dimensional perfectly conducting cylinder in slab medium, *Journal of Electronic Imaging* **19** (Dec 2010), 043016.
[25] C.H. Sun and C.C. Chiu, Electromagnetic imaging of buried perfectly conducting cylinders targets using the dynamic differential evolution, *International Journal of RF and Microwave Computer-Aided Engineering* **22**(2) (Mar 2012), 141–146.
[26] C.C. Chiu and W.C. Hsiao, Comparison of asynchronous particle swarm optimization and dynamic differential evolution for partially immersed conductor, *Waves in Random and Complex Media* **21**(3) (Aug 2011), 485–500.
[27] I.T. Rekanos, Shape reconstruction of a perfectly conducting scatterer using differential evolution and particle swarm optimization, *IEEE Transactions on Geoscience and Remote Sensing* **46**(7) (Jul 2008), 1967–1974.
[28] C.H. Huang, C.C. Chiu, C.L. Li and K. C. Chen, Time domain inverse scattering of a two-dimensional homogenous dielectric object with arbitrary shape by particle swarm optimization, *Progress in Electromagnetic Research* **82** (February 2008), 381–400.
[29] C.H. Sun, C.C. Chiu and C.L. Li, Time-domain inverse scattering of a two- dimensional metallic cylinder in slab medium using asynchronous particle swarm optimization, *Progress in Electromagnetic Research M* **14** (Aug 2010), 85–100.
[30] W. Chien, C.C. Chiu, C.L. Li and C.H. Sun, Microwave imaging of a partially immersed non-uniform conducting cylinder, *International Journal of Applied Electromagnetics and Mechanics* **40** (Dec 2012), 215–225.
[31] C.C. Chiu and Y.W. Kiang, Electromagnetic imaging for an imperfectly conducting cylinder, *IEEE Transactions on Microwave Theory and Techniques* **39** (Sept 1991), 1632–1639.
[32] L. Pan, Y. Zhong, X. Chen and S.P. Yeo, Subspace-based optimization method for inverse scattering problems utilizing phaseless data, *IEEE Transactions on Geoscience and Remote Sensing* **49**(3) (Mar 2011), 981–981.
[33] K.C. Lee, A neural-network-based model for 2D microwave imaging of cylinders, *International Journal of RF and Microwave Computer-Aided Engineering* **4**(5) (Sept 2004), 398–403.
[34] M.R. Hajihashemi and M.E. Shenawee, TE versus tm for the shape reconstruction of 2-D pec targets using the level-set algorithm, *IEEE Transactions on Geoscience and Remote Sensing* **48**(3) (Mar 2010), 1159–1168.
[35] C.C. Chiu and W.-T. Chen, Inverse scattering of a buried imperfect conductor by the genetic algorithm, *International Journal of Imaging Systems and Technology* **11** (2000), 35–360.
[36] C.C. Chiu and W.-T. Chen, Electromagnetic imaging for an imperfectly conducting cylinder by the genetic algorithm, *IEEE Tans Microwave Theory Tech* **48**(11) (2000), 1901–1905.
[37] M. Benedetti, M. donelli and A. Massa, Multicrack detection in two-dimensional structures by means of ga-based strategies, *IEEE Transactions on Antennas and Propagation* **55**(1) (Jan 2007), 205–215.
[38] A. Qing, Electromagnetic inverse scattering of multiple perfectly conducting cylinders by differential evolution strategy with individuals in groups (GDES), *Antennas and Propagation, IEEE Transactions on* **52**(5) (2004), 1223–1229.
[39] C.H. Huang, H.C. Lu, C.C. Chiu, T. Wysocki and B.J. Wysock, Image reconstruction of buried multiple conductors by genetic algorithms, *International Journal of Imaging Systems and Technology* **18** (Oct 2008), 276–281.
[40] M. Clerc, The swarm and the queen: Towards a deterministic and adaptive particle swarm optimization, *Proceedings of Congress on Evolutionary Computation*, Washington, DC, (1999), 1951–1957.
[41] C.L. Li, S.H. Chen, C.M. Yang and C.C. Chiu, Electromagnetic imaging for a partially immersed perfectly conducting cylinder by the genetic algorithm, *Radio Science* **39**(2) (April 2004), RS2016.

[42] W. Chien and C.C. Chiu, Using nu-ssga to reduce the searching time in inverse problem of a buried metallic object, *IEEE Transactions on Antennas and Propagation* **53**(10) (October 2005), 3128–3134.
[43] A. Carlisle and G. Dozier, An off-the-shelf PSO, *Proceedings of the 2001 Workshop on Particle Swarm Optimization* (2001), 1–6.